

RESEARCH ARTICLE

Open Access



MicroRNA-9 induces defective trafficking of Nav1.1 and Nav1.2 by targeting Nav β 2 protein coding region in rat with chronic brain hypoperfusion

Li-Hua Sun^{1*}, Mei-Ling Yan¹, Xue-Ling Hu¹, Li-Wei Peng¹, Hui Che¹, Ya-Nan Bao¹, Fei Guo¹, Tong Liu¹, Xin Chen¹, Rong Zhang¹, Tao Ban¹, Ning Wang¹, Huai-Lei Liu², Xu Hou² and Jing Ai^{1*}

Abstract

Background: Previous studies have demonstrated that the trafficking defects of Nav1.1/Nav1.2 are involved in the dementia pathophysiology. However, the detailed mechanisms are not fully understood. Moreover, whether the impaired miRNAs regulation linked to dementia is a key player in sodium channel trafficking disturbance remains unclear. The cognitive impairment induced by chronic cerebral ischemia through chronic brain hypoperfusion (CBH) is likely reason to precede dementia. Therefore, our goal in the present study was to examine the role of microRNA-9 (miR-9) in regulating Nav1.1/Nav1.2 trafficking under CBH generated by bilateral common carotid artery occlusion (2VO).

Results: The impairment of Nav1.1/Nav1.2 trafficking and decreased expression of Nav β 2 were found in the hippocampi and cortices of rats following CBH generated by bilateral 2VO. MiR-9 was increased in both the hippocampi and cortices of rats following CBH by qRT-PCR. Intriguingly, miR-9 suppressed, while AMO-miR-9 enhanced, the trafficking of Nav1.1/Nav1.2 from cytoplasm to cell membrane. Further study showed that overexpression of miR-9 inhibited the Nav β 2 expression by targeting on its coding sequence (CDS) domain by dual luciferase assay. However, binding-site mutation or miR-masks failed to influence Nav β 2 expression as well as Nav1.1/Nav1.2 trafficking process, indicating that Nav β 2 is a potential target for miR-9. Lentivirus-mediated miR-9 overexpression also inhibited Nav β 2 expression and elicited translocation deficits to cell membrane of Nav1.1/Nav1.2 in rats, whereas injection of lentivirus-mediated miR-9 knockdown could reverse the impaired trafficking of Nav1.1/Nav1.2 triggered by 2VO.

Conclusions: We conclude that miR-9 may play a key role in regulating the process of Nav1.1/Nav1.2 trafficking via targeting on Nav β 2 protein in 2VO rats at post-transcriptional level, and inhibition of miR-9 may be a potentially valuable approach to prevent Nav1.1/Nav1.2 trafficking disturbance induced by CBH.

Keywords: microRNA-9, Chronic brain hypoperfusion, Sodium channel

* Correspondence: sunlihua0219@163.com; aijing@ems.hrbmu.edu.cn

¹Department of Pharmacology, Harbin Medical University, No.157 Baojian Road, Nangang District, Harbin, Heilongjiang Province 15008, China
Full list of author information is available at the end of the article

Background

Since voltage-gated sodium channel (VGSC) is necessary in the initiation and propagation of action potentials in neurons, it is a valuable therapeutic target for neurological disorders, such as epilepsy and chronic neuropathic pain [1–3]. Recent studies have now expanded the role of sodium channels in multi-neurological diseases including autism, migraine and multiple sclerosis [2, 4, 5]. A prospective study reported that Alzheimer's disease (AD) have an increased risk of developing seizures and epilepsy [6]. A recent study reported that over activity of hippocampus might contribute to AD-related cognitive decline [7] and antiepileptic drug was demonstrated to reverse cognitive deficits and diminished the anxiety phenotypes in AD mice [8]. And electrical imbalance may contribute to cognitive deficits in AD and serve as a target for clinical intervention [9, 10]. These studies together suggest that dysfunction of VGSC may share the common phenotype between AD and epilepsy.

Voltage-gated Na⁺ channels (VGSCs) are macromolecular protein complexes, which are composed of α -subunits (Nav1.1–Nav1.9) and β -subunits (Nav β 1, Nav β 1B, Nav β 2, Nav β 3 and Nav β 4), in which α -subunits are necessary for forming a functional ion-selective channel and β -subunits affect ion channel gating and trafficking to regulate the voltage-dependency and density of VGSC on the cell membrane. It has been reported that mutation of Nav1.1, a remarkable feature of Dravet syndrome, could induce higher seizure activity and cognitive dysfunction [11]. Interestingly, Nav1.1 retained inside the cells while its expression reduces markedly in *BACE1*-transgenic mice, accompanied with disturbed Nav β 2 [12]. And restoring Nav1.1 level could reduce memory deficits in human amyloid precursor protein (*hAPP*) transgenic mice [13]. Furthermore, elevated cell surface Nav1.2 expression contributes to the epileptic behaviors in *BACE1*-null mice [14]. These studies indicated that the abnormal Nav1.1/Nav1.2 trafficking may be involved in dementia. Nav β 2 plays a key role in the trafficking of α -subunits from cytoplasm to cell membrane [15–17], and keeping the steady-state stabilization of VGSC complexes at the plasma membrane [18]. Interestingly, Nav β 2 is also one substrate for beta-secretase (*BACE1*) in *BACE1*-deficient or over-expressing mice [19], and the increased Nav β 2 cleavage contributes to aberrant neuronal activity and cognitive deficits in amyloid precursor protein (*APP*) mice [20]. However, the mechanism remains largely unclear.

Chronic brain hypoperfusion (CBH)-mediated chronic cerebral ischemia and consequent cognitive impairment [21, 22] is most likely to precede dementia [23, 24]. It has been reported that CBH not only induces the accumulation of beta-amyloid (A β) [21, 24] and cell death [25], but also reduces dendritic arborizations as well as synaptic contacts [26]. And acute cerebral ischemia by the

occlusion of right middle cerebral artery downregulates the total Nav1.1 protein expression from 6 h to 2 days, which was further increased from 3 to 7 days [27]. However, whether and how CBH influences the expression or trafficking of Nav1.1/Nav1.2 has not been reported.

MicroRNAs are small non-coding RNA, which regulate protein synthesis. MicroRNA-9 (miR-9), enriched in central nerve system (CNS) [28], contributes likely to multi-pathological processes including the neurogenesis [29], proliferation [30], migration and differentiation of neural progenitor cells [31], drug adaptation [32], adult brain plasticity [33], neural cell fate [34], the migration and proliferation of glioma cells [35], axon extension and branching [36], spinal motor neuron development [37] under physiological status. Importantly, miR-9 expression has been downregulated in the brain of patients with Huntington's disease [38] and up-regulated in the patients with Alzheimer's disease [39], suggesting that abnormal expression of miR-9 may be involved at least partially in the processes of neurodegenerative diseases. Therefore, whether and how miR-9 participates in the abnormal expression or trafficking of Nav1.1/Nav1.2 induced by CBH is worth to be explored.

In this study, our data provide strong evidence that miR-9 regulates Nav1.1/Nav1.2 trafficking by post-transcriptional regulating *SCN2B* gene under CBH status.

Results

CBH-mediated Nav1.1/Nav1.2 trafficking defect in the hippocampi and cortices

Previous studies have reported that Nav1.1/Nav1.2 trafficking was changed after dementia [19, 20, 40]. Since the functional protein of Nav1.1/Nav1.2 located in the membrane, we first evaluated the surface expression of Nav1.1/Nav1.2 and found that the surface expression of Nav1.1 and Nav1.2 was reduced both in the hippocampi and cortices of 2VO rats (Fig. 1a, $P < 0.01$ vs sham). In order to explore whether the decreased surface protein expression of Nav1.1/Nav1.2 was due to the reduction of total Nav1.1/Nav1.2 or the impairment of trafficking, the total protein levels of Nav1.1/Nav1.2 were evaluated. The data showed that the total protein levels of Nav1.1 and Nav1.2 were significantly increased in the hippocampi and cortices of 2VO rats (Fig. 1b, $P < 0.01$ vs sham) rather than reduced. These results suggested that the decreased expression of Nav1.1/Nav1.2 on the cell membrane were due presumably to the impaired trafficking of Nav1.1 and Nav1.2 protein from cytoplasm to cell membrane in 2VO rats rather than the changes of their total protein levels.

CBH-mediated Nav β 2 downregulation in hippocampi and cortices

Since Nav β 2 is considered as an important regulator for trafficking Nav1.1/Nav1.2 upon reports from others

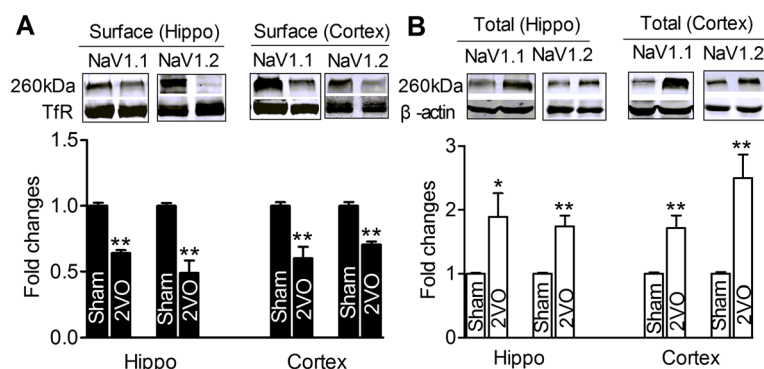


Fig. 1 Nav1.1 and Nav1.2 trafficking were disturbed in hippocampi and cortices after chronic brain hypoperfusion (CBH). **a**, western-blot analysis of the surface protein levels of Nav1.1 and Nav1.2 in sham and 2VO rats, upper: representative immunoblots of Nav1.1 and Nav1.2; lower: the quantitative analysis data of the immunoblots. The optical density was evaluated for each band and values for 2VO rat tissue were normalized to sham group after correction for protein loading with TfR, ** $P < 0.01$ vs sham, mean \pm s.e.m, $n = 6$. **b**, western-blot analysis of the total protein levels of Nav1.1 and Nav1.2 in sham and 2VO rats, upper: representative immunoblots of Nav1.1, Nav1.2; lower: the quantitative analysis data of the immunoblots. The optical density was evaluated for each band and values for 2VO rat tissue were normalized to sham group after correction for protein loading with β -actin. ** $P < 0.01$ vs sham, mean \pm s.e.m, $n = 6$

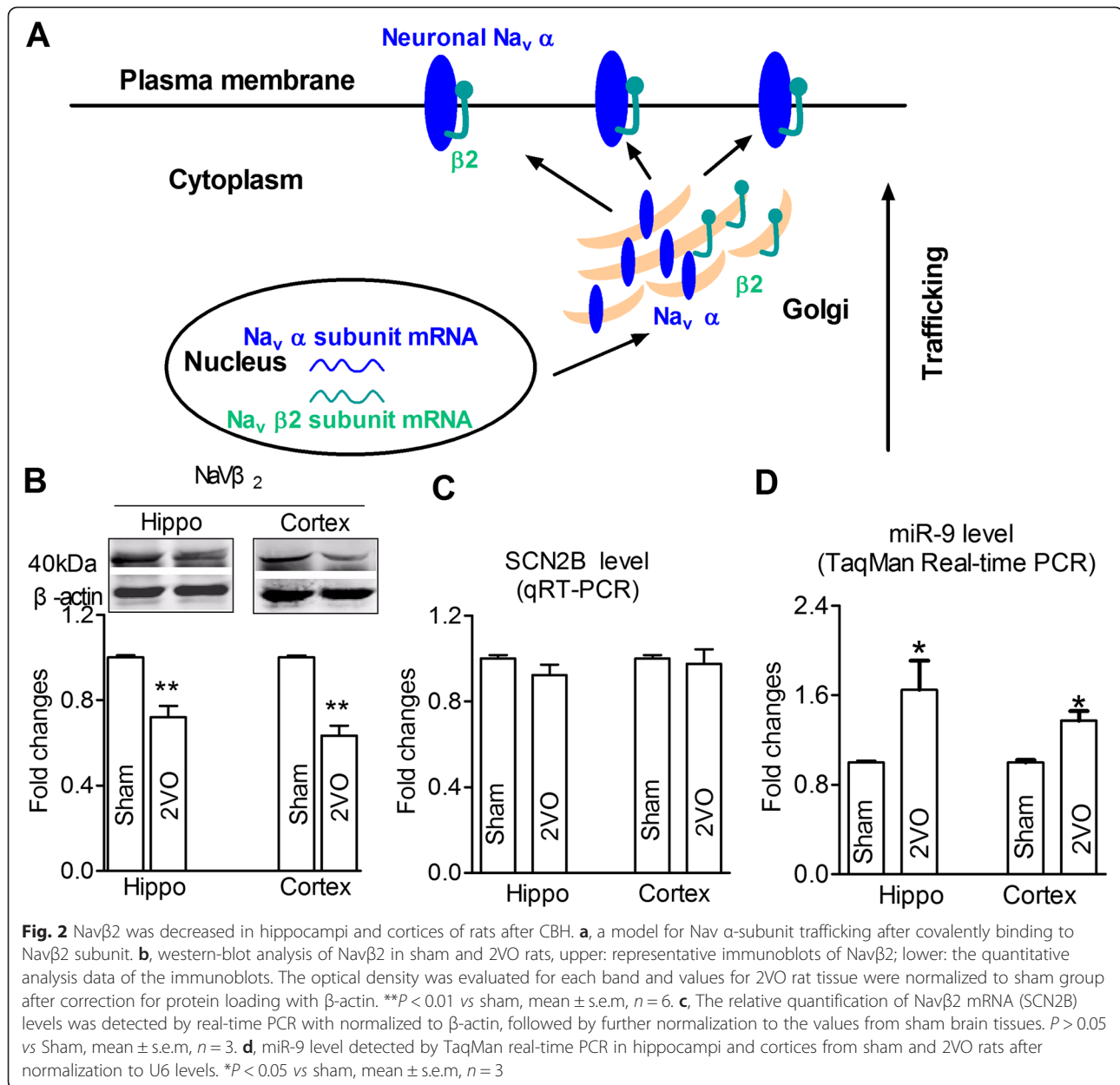
[16, 17] and our current observation (Fig. 2a), we then investigate the expression of Nav β 2 in either hippocampus or cortex of 2VO rats. The protein expression of Nav β 2 was significantly decreased in both brain locations compared with that in sham rats (Fig. 2b, $P < 0.01$). However, their mRNA expression of Nav β 2 (SCN2B) was not changed consistently with the protein expression of Nav β 2 (Fig. 2c), suggesting that this may be ascribed to the post-transcriptional regulation.

MiR-9-mediated post-transcriptional regulation of Nav β 2 expression

MicroRNAs have long been known to control post-transcriptional gene regulation and are essential for neuronal function [41]. MiR-9 is enriched in CNS, and increases in the brain of the patients with Alzheimer's disease (AD) [39]. To test potential involvement of miR-9 in CBH-mediated 2VO rats, we also evaluated the expression of miR-9 in hippocampi and cortices of 2VO rats. Surprisingly, the expression levels in both brain regions were significantly increased compared with those in sham control rats quantified using qRT-PCR (Fig. 2d, $P < 0.05$).

Since the protein level of Nav β 2 was reduced in both hippocampi and cortices in 2VO rats, which is discrepancy with the unchanged SCN2B expression, the alternation of miR-9 is highly expected in this process. By searching the database of microRNA targets (<http://www.targetscan.org/>), we found that SCN2B has a poorly conservative 'seed' sequence of miR-9 in its 3'UTR and the length of 3'UTR of SCB2B in rat was very short based on the database of the University of California Santa Cruz (UCSC) and the National Center

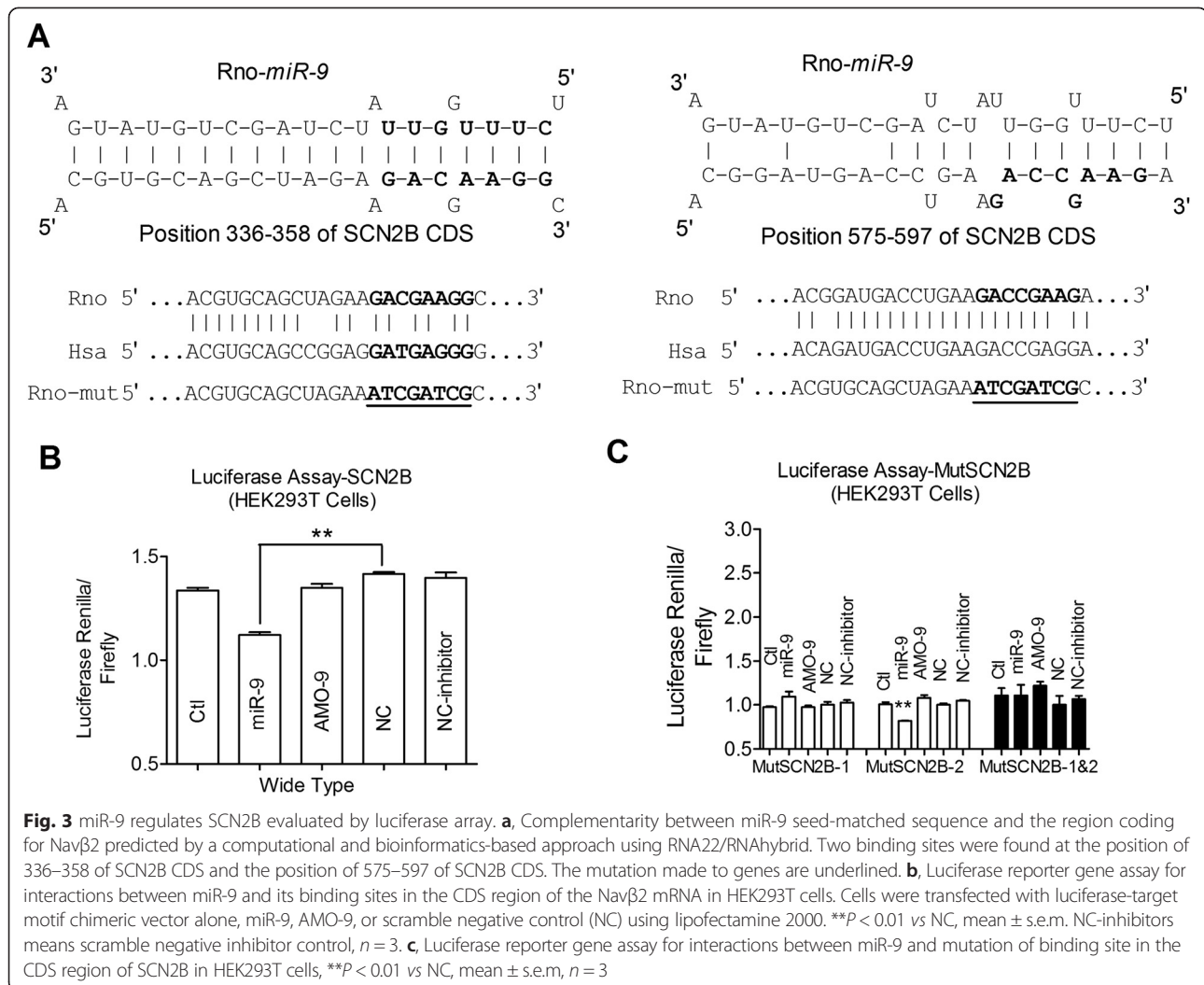
for Biotechnology Information (NCBI) Genome Browsers. Since recent studies have reported that microRNAs regulate protein expression by binding to the coding regions of target protein [41–43], we then searched RNA22/RNA hybrid (<http://bibiserv.techfak.uni-bielefeld.de/rnahybrid/>) and found that the CDS domain of SCN2B is likely to serve as potential targets for miR-9. We next identified whether there are binding sites for miR-9 on the CDS domain of SCN2B gene at the position of 336–358 and 575–597 with highly conservative regions (Fig. 3a). We subsequently screened the predicted SCN2B binding sites using luciferase assays (see Methods) and then selected constructs including position 336–358 and position 575–597 of SCN2B CDS domains that substantially suppressed luciferase expression in the presence of the matching microRNAs (Fig. 3b). MiR-9 inhibited the SCN2B-CDS luciferase activity compared with scrambled negative control (Fig. 3b, $P < 0.01$), however, scrambled negative control and inhibitor of miR-9 had no effect on luciferase activity compared with control group (Fig. 3b, $P > 0.05$), and the difference of luciferase activity between inhibitor of miR-9 and scramble negative inhibitor control was also not detected (Fig. 3b, $P > 0.05$). For each of the two binding sites, we generated and tested several variants by introducing silent mutations designed to disrupt the putative base pairings between the microRNAs and the corresponding predicted targets. Silent mutations introduced into the predicted targets at the position of 336–358 of SCN2B CDS disrupted the ability of miR-9 to repress the translation of the SCN2B-CDS (Fig. 3c, $P < 0.01$). However, simultaneous introduction of silent mutations at the position of 575–597 of SCN2B CDS did not abolish the



downregulation of SCN2B by miR-9 (Fig. 3c, $P > 0.05$). Silent mutations introduced into both two predicted targets at the positions of 336–358 and 575–597 of SCN2B CDS, MutSCN2B-1 & 2 disrupted the ability of miR-9 to repress the translation of the SCN2B-CDS, strongly suggesting that miR-9 uniquely targets at the position of 336–358, rather than 575–597, of SCN2B CDS.

To observe the influence of miR-9 on the protein translation of SCN2B, we analyzed the protein levels of Nav $\beta 2$ in primary cultured neonatal rat neurons (NRNs) co-transfected with miR-9 mimics. The successful transfection of miR-9 was identified (Fig. 4a) by

qRT-PCR and Nav $\beta 2$ protein levels were significantly decreased in the presence of miR-9 (Fig. 4b). AMO-9 rescued the downregulation of Nav $\beta 2$ elicited by overexpression of miR-9 and scrambled negative control of microRNA failed to affect the protein levels, suggesting that miR-9 predominantly suppresses SCN2B translation (Fig. 4b,d). However, the mRNA level of Nav $\beta 2$ was not changed in the presence of miR-9 (Fig. 4c), which may ascribed to transcriptional regulation. To verify the transcriptional mechanism of miR-9 on Nav $\beta 2$, the target protector technique was applied and the results showed that the SCN2B target protector



(oligodeoxynucleotides (ODNs)-miR) of miR-9 (the position of 336–358 of SCN2B CDS) attenuated the reduction in Navβ2 levels induced by miR-9 (Fig. 4e, $P < 0.01$), implying that the SCN2B shows a great potential as the target for miR-9.

MiR-9-induced increase of total Nav1.1 /Nav1.2 protein in vitro

To test the trafficking effect of miR-9 on Nav1.1/Nav1.2, the protein expressions of Nav1.1 and Nav1.2 after pretreatment of NRNs with miR-9 were detected by both Western blot and immunofluorescence techniques. The results showed that miR-9 significantly increased the expression of Nav1.1 (Fig. 5a, $P < 0.05$) and Nav1.2 (Fig. 5b, $P < 0.05$) total protein. And they were prevented in the presence of AMO-9 (Fig. 5a,b). The results were further observed by immunofluorescent analysis (Fig. 5c,d).

MiR-9-induced disturbances of Nav1.1/Nav1.2 trafficking in vivo

To verify the functional role of miR-9 on Nav1.1/Nav1.2 trafficking *in vivo*, miR-9 oligonucleotide carried by lentivirus vector (lenti-pre-miR-9) was injected directly into CA1 region of bilateral hippocampus of each rat and significantly higher expression of miR-9 in both hippocampi and cortices was observed at 8 weeks after injection compared with the negative control oligonucleotide (NC, Fig. 6a). Importantly, the expression of Navβ2 was also significantly decreased at meantime in lenti-pre-miR-9 group compared with control group, which was reversed by lenti-pre-AMO-miR-9 (Fig. 6b, $P < 0.01$). The surface expressions of both Nav1.1 and Nav1.2 proteins were markedly reduced in both hippocampi and cortices of rats with lenti-pre-miR-9 treatment, which was reversed by lenti-pre-AMO-miR-9 (Fig. 6c-f, $P < 0.05$), even though the total protein levels of Nav1.1 and Nav1.2 were increased in

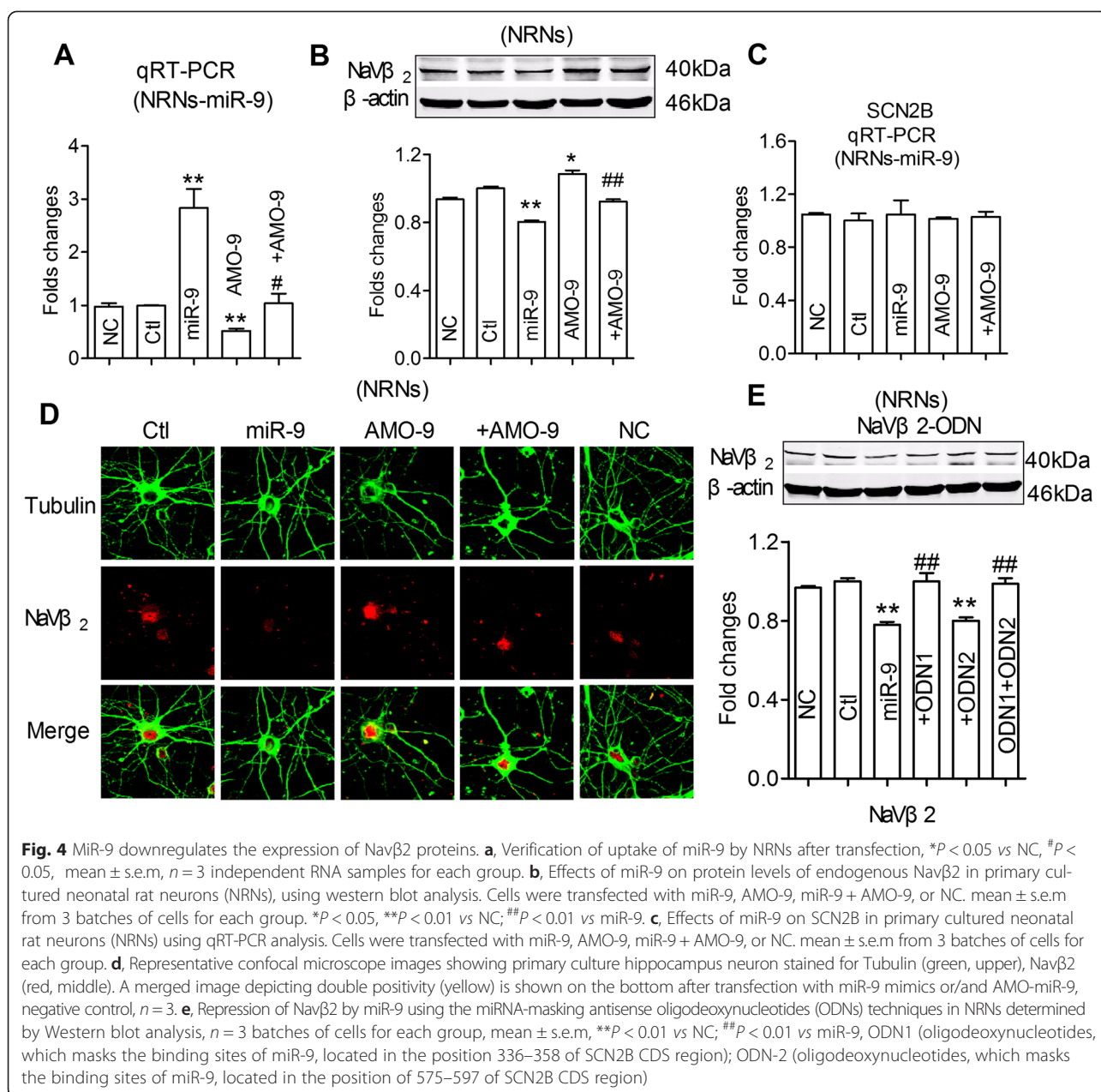


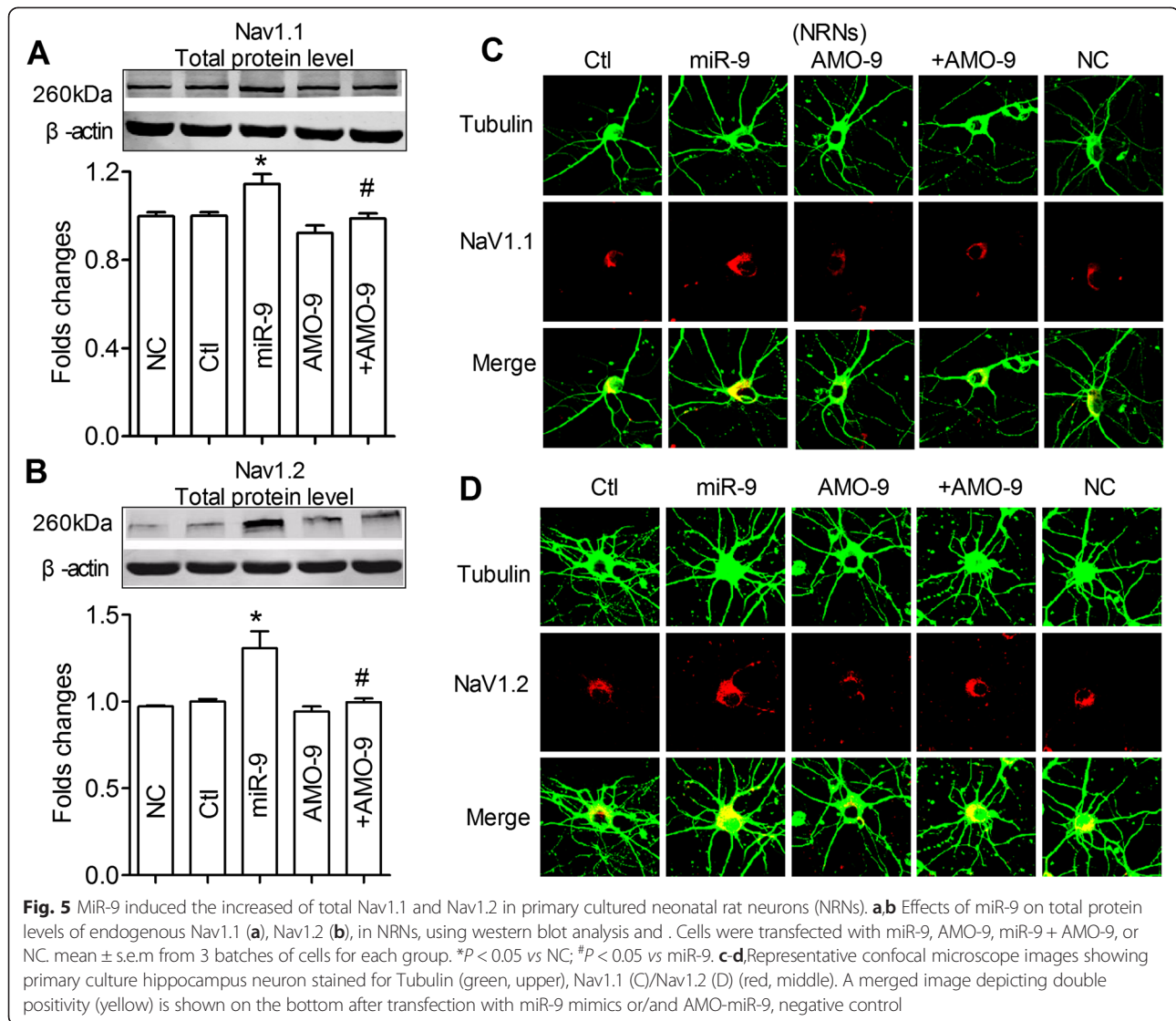
Fig. 4 MiR-9 downregulates the expression of Navβ2 proteins. **a**, Verification of uptake of miR-9 by NRNs after transfection, * $P < 0.05$ vs NC, # $P < 0.05$, mean \pm s.e.m, $n = 3$ independent RNA samples for each group. **b**, Effects of miR-9 on protein levels of endogenous Navβ2 in primary cultured neonatal rat neurons (NRNs), using western blot analysis. Cells were transfected with miR-9, AMO-9, miR-9 + AMO-9, or NC. mean \pm s.e.m from 3 batches of cells for each group. * $P < 0.05$, ** $P < 0.01$ vs NC; ## $P < 0.01$ vs miR-9. **c**, Effects of miR-9 on SCN2B in primary cultured neonatal rat neurons (NRNs) using qRT-PCR analysis. Cells were transfected with miR-9, AMO-9, miR-9 + AMO-9, or NC. mean \pm s.e.m from 3 batches of cells for each group. **d**, Representative confocal microscope images showing primary culture hippocampus neuron stained for Tubulin (green, upper), Navβ2 (red, middle). A merged image depicting double positivity (yellow) is shown on the bottom after transfection with miR-9 mimics or/and AMO-miR-9, negative control, $n = 3$. **e**, Repression of Navβ2 by miR-9 using the miRNA-masking antisense oligodeoxynucleotides (ODNs) techniques in NRNs determined by Western blot analysis, $n = 3$ batches of cells for each group, mean \pm s.e.m, *** $P < 0.01$ vs NC; ## $P < 0.01$ vs miR-9, ODN1 (oligodeoxynucleotides, which masks the binding sites of miR-9, located in the position 336–358 of SCN2B CDS region); ODN-2 (oligodeoxynucleotides, which masks the binding sites of miR-9, located in the position of 575–597 of SCN2B CDS region)

both hippocampi and cortices of rats with lenti-pre-miR-9 treatment, which were reversed by lenti-pre-AMO-miR-9 (Fig. 6c-f, $P < 0.05$). These data suggested that miR-9 plays an important role in trafficking and cellular distribution of Nav1.1/ Nav1.2.

Reversal effect of AMO-miR-9 on trafficking defects of Nav1.1/Nav1.2 induced by 2VO

Our data displayed that 2VO results in miR-9 increase, and over-expression of miR-9 then induces the trafficking defects of Nav1.1/Nav1.2 in vitro. In order to evaluate the protective effect of AMO-miR-9 on the

onset of the trafficking defects of Nav1.1/Nav1.2 in 2VO rats, lenti-pre-AMO-miR-9 was injected into the hippocampus area. At 8 weeks after injection, miR-9 level was significantly decreased in both hippocampi and cortices compared with 2VO rats (Fig. 7a). To our interest, the decreased expression of Navβ2 was also reversed by lenti-pre-AMO-miR-9 treatment in the same brain regions (Fig. 7b, $P < 0.01$). And furthermore, the surface protein expression of Nav1.1 was increased and the total protein of Nav1.1 level was decreased by lenti-pre-AMO-miR-9 compared with that in 2VO control rats (Fig. 7c,d, $P < 0.05$). Similarly, lenti-pre-AMO-



miR-9 effectively improved the impaired trafficking of Nav1.2 from cytoplasm to cell membrane under the same experimental condition (Fig. 7e and f, $P < 0.05$).

Discussion

In this study, our observations have demonstrated, for the first time that CBH induces the trafficking defects of Nav1.1/Nav1.2 in hippocampi and cortices areas in 2VO rats, leading to the decrease in the expression of Nav β 2 protein. Further study has shown that the increased miR-9 negatively regulated the expression of Nav β 2 protein by binding to the target in CDS region of SCN2B gene. This observation provides a novel mechanism to modify the reduction in Nav1.1/Nav1.2 membrane trafficking, and careful monitoring the changes in miR-9 level and the expression for Nav1.1/

Nav1.2 and targeted gene are considerably necessary during CBH.

Molecular identity and trafficking characters of Nav1.1/Nav1.2 in rat brain after CBH

It has been known that Nav1.1, Nav1.2, and Nav1.6 are abundant in the central nervous system, whereas Nav1.3 is mostly present during embryonic stage [44]. Nav1.6 is concentrated in the axon initial segment (AIS) nodes of Ranvier and in proximal dendrites in many types of neurons [45]. Since cell surface levels of Nav1.1 and Nav1.2 subunits dramatically decrease in the brains of *BACE1*-transgenic mice although total Nav1.1 and Nav1.2 levels are elevated [12, 14], and that the axonal and surface levels of Nav1.2 are significantly increased in hippocampal neurons from *BACE1*-null mice [7]. In the present study, the expression of Nav1.1

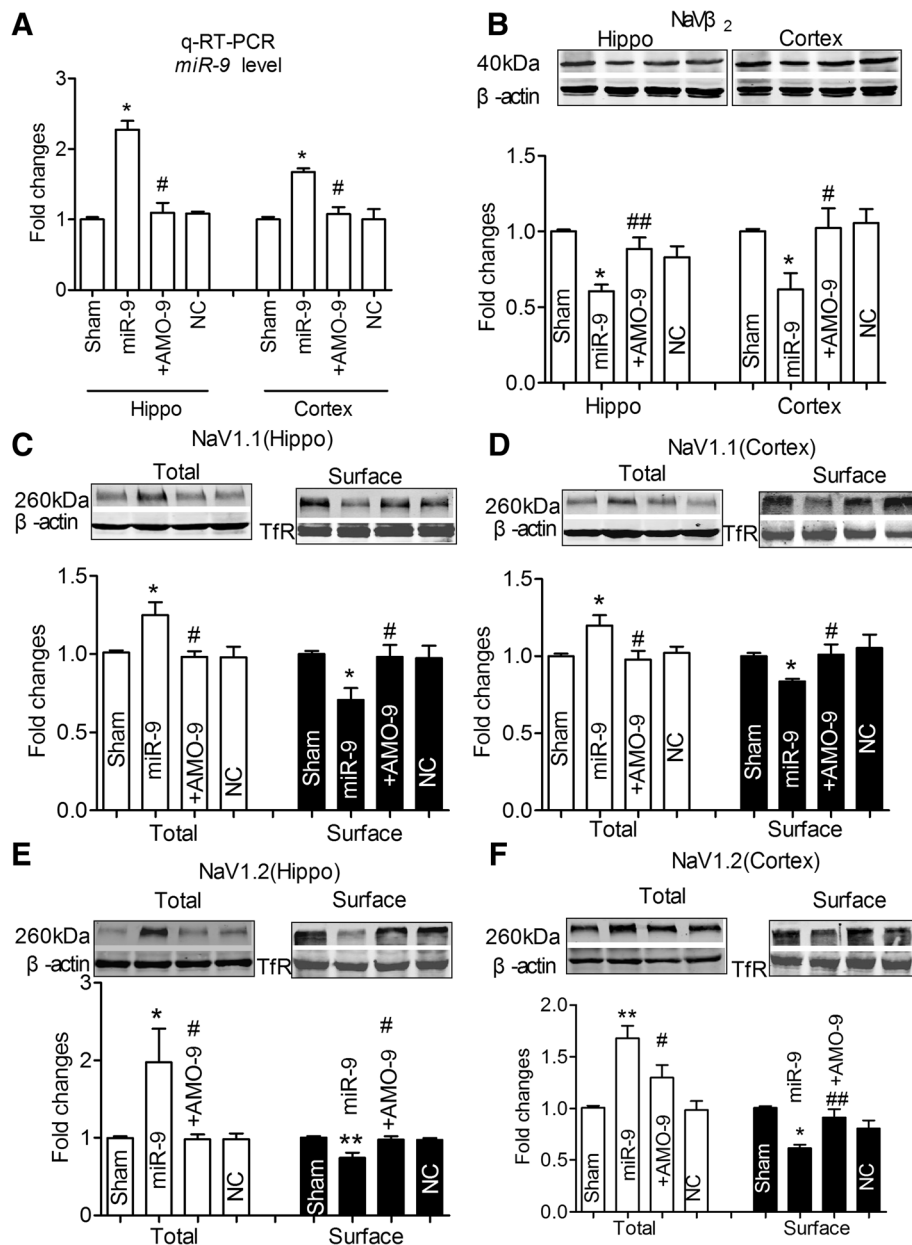


Fig. 6 MiR-9 produces the disturbance of trafficking, cellular distribution of Nav1.1 and Nav1.2 in rats. **a**, Detection of miR-9 in hippocampi and cortices tissues after stereotaxic injection 8 weeks using qRT-PCR. Rats were transfected with lenti-pre- miR-9, lenti-pre-miR-9 + lenti-pre-AMO-miR-9, or NC. Data was shown by mean \pm s.e.m from 6 rats for each group. * $P < 0.05$ vs NC; # $P < 0.05$ vs lenti-pre- miR-9. **b**, Navβ₂ protein expressions in hippocampi and cortices tissues after treatment by lenti-pre-miR-9, lenti-pre-miR-9 + lenti-pre-AMO-miR-9, or NC for 8 weeks. **c-f**, Nav1.1 (C-D), Nav1.2 (E-F) total and surface protein expressions in hippocampi and cortices tissues after treatment by lenti-pre-miR-9, lenti-pre-miR-9 + lenti-pre-AMO-miR-9, or NC for 8 weeks. * $P < 0.05$, ** $P < 0.01$ vs NC; # $P < 0.05$, ## $P < 0.01$ vs lenti-pre- miR-9, mean \pm s.e.m, $n = 6$

and Nav1.2 of both surface and total protein were detected in hippocampi and cortices of rat following CBH and our data showed that CBH could induce trafficking defects of Nav1.1/Nav1.2 with significant increase in total protein levels of Nav1.1/Nav1.2 and the marked decrease in surface protein levels of Nav1.1/Nav1.2.

The results are consistent with previous study performed using *BACE1*-transgenic mice [12].

Previous studies have demonstrated that Navβ₂ subunit, an auxiliary subunit of Nav channel, participates in channel trafficking, re-localization, and interaction of both Nav1.1 [46, 47] and Nav1.2 [45]. Importantly, a

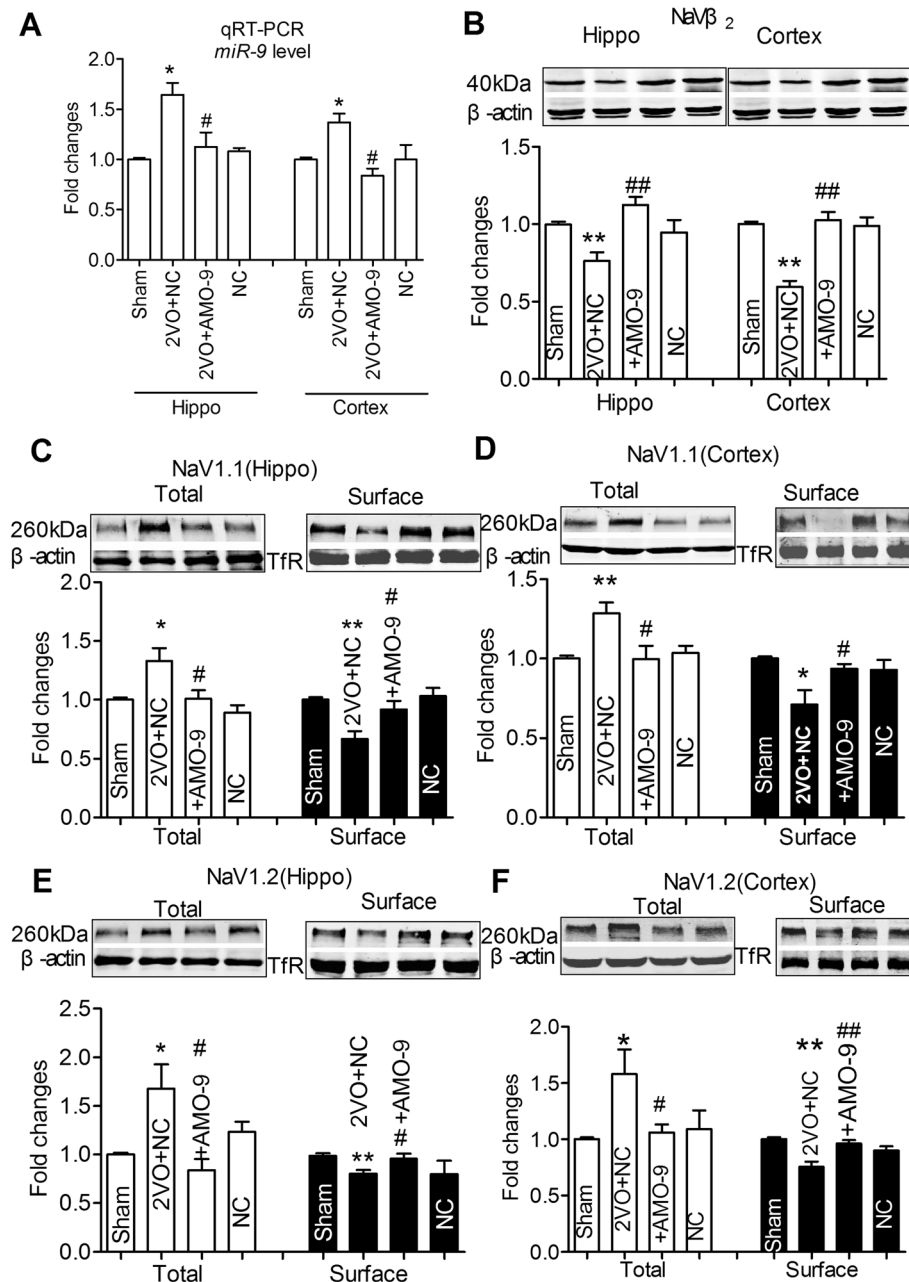


Fig. 7 AMO-miR-9 prevented the disturbed trafficking of Nav1.1/Nav1.2 induced by 2VO. **a**, Detection of miR-9 in hippocampi and cortices tissues after stereotaxic injection 8 weeks using qRT-PCR. 2VO rats were transfected with lenti-pre-AMO-miR-9, or NC. Data was shown by mean \pm s.e.m from 6 rats for each group. * $P < 0.05$ vs sham; # $P < 0.05$ vs 2VO. **b**, Navβ₂ protein expressions in hippocampi and cortices tissues in 2VO rats with or without lenti-pre-AMO-miR-9 treatment, or NC for 8 weeks. **c-f**, Nav1.1 (C-D), Nav1.2 (E-F) total and surface protein expressions in 2VO rats with or without lenti-pre-AMO-miR-9 treatment, or NC for 8 weeks. * $P < 0.05$, ** $P < 0.01$ vs sham; # $P < 0.05$, ## $P < 0.01$ vs 2VO, mean \pm s.e.m, $n = 6$

recent study has also shown that the abnormal Navβ₂ cleavage mediated by *BACE1* affects Nav1.1 and Nav1.2 surface trafficking differentially [48]. Furthermore, in AD status, the intracellular domain of Navβ₂ functionally regulates the α-subunit of VGSCs and the elevated *BACE1* activity leading to decrease in surface levels of Nav1.1 in neuronal cells [49]. Interestingly, here we

found that CBH not only impaired Nav1.1/Nav1.2 trafficking in rat hippocampi and cortices, but also down-regulated the expression of Navβ₂, suggesting Navβ₂ may be more likely involved in the abnormal trafficking of both Nav1.1 and Nav1.2 induced by CBH. Of noted, previous studies have demonstrated that 2VO provokes chronic brain hypoxia and triggers spatial memory

impairment in rats accompanied with elevation of *APP* and *BACE1* expression [24, 41]. Whether the impaired trafficking of Nav1.1/ Nav1.2 in the present study is associated with CBH induced high level of *APP* and *BACE1* is unknown and need to be elucidated further.

Negative regulation of miR-9 on Nav β 2 protein-mediated trafficking disturbance of Nav1.1/Nav1.2 in vitro

As far as we know, microRNAs are newly discovered and commonly considered as modulators of protein expression at post-transcriptional level, which are associated with the pathogenesis in multiple kinds of diseases [50–53]. In the present study, our observations have shown that the mRNA level for Nav β 2 unaltered in hippocampi and cortices of 2VO rat but its targeted protein expression significantly decreased (Fig. 2b), indicating that the post-transcriptional regulation must be existed to modify Nav β 2 expression. It has been documented in the literature that miR-9 is elevated in hippocampus [39] and temporal lobe cortex [54] of AD patients, whereas, the opposite observation is also presented in AD patients [55] from others, which was then demonstrated downregulation of miR-9 due to overexpression of A β in hippocampal cultures [56]. The discrepancies imply that the changes in miR-9 in AD depend presumably upon the variants inducers. In the present study, The major finding is that miR-9 is significantly up-regulated under CBH conditions in animal model (Fig. 2d).

Our study provides strong evidences that miR-9 increases in both hippocampi and cortices, and inhibited the expression of Nav β 2, which in turn blocked the trafficking of Nav1.1 and Nav1.2 from cytoplasm to plasma membrane (Figs. 3, 4 and 5). However, why the total Nav1.1/Nav1.2 protein levels increase in cultured neuron following miR-9 treatment and how 2VO triggers Nav1.1/Nav1.2 total protein up-regulation remain unclear. The possible explanation may be due at least partially to a unknown mechanism increasing protein synthesis to compensate the trafficking defect-mediated the decrease in surface expression of Nav1.1/Nav1.2. But the detailed mechanism needs to be further studied.

In addition, our important finding here is that miR-9 regulates endogenous Nav β 2 expression by targeting its coding sequence (CDS) region rather than not 3'UTR of SCN2B (Fig. 4). Additionally, another evidence collected from the current investigation demonstrate that the microRNA-mediated regulation is not limited to the 3'UTR, the functionality of target sites in the CDS also confirmed by previous studies [57–59], such as miR-24 [58], miR-296, miR-470, miR-134 [60], miR-126 [43], miR-181a [59], miR-148 [57] and miR-519 [61] that target sequences within the mRNA coding region have been reported to repress the biosynthesis of the encoded proteins in similar way. Our results provided another

evidence that, microRNA-mediated regulation is not limited to target on the 3'UTR of genes, the functionality of target sites is also located in the CDS domain.

Negative regulation of miR-9 on Nav β 2 protein-mediated trafficking defects of Nav1.1/Nav1.2 in vivo

More importantly, our *in vivo* study supports the data collected from our *in vitro* observations that the upregulation of miR-9 induced by both CBH and lenti-pre-miR-9 could also disturb the trafficking of both Nav1.1/ Nav1.2 by downregulation of Nav β 2 expression. On the contrary, lenti-pre-AMO-miR-9 injection into hippocampus markedly prevents the abnormal trafficking of both Nav1.1 and Nav1.2 following either CBH or lenti-pre-miR-9 treated normal rats accompanied by increased Nav β 2 expression. These results combination with our *in vitro* data suggested that the inhibition of miR-9 in hippocampi and cortices in CBH model rats would be a way to prevent sodium channel dysfunction after CBH. An understanding of miR-9-Nav β 2-Nav1.1/Nav1.2 trafficking pathway could yield to the potential therapeutic targets for the prevention of abnormal electrical activation induced by CBH.

Limitation and prospect

In the present study, though we have demonstrated the regulation effect of miR-9 on the trafficking of Nav1.1/ Nav1.2 by inhibiting the expression of Nav β 2 both *in vitro* and *in vivo*, we did not provide evidence whether these changes could induce abnormal sodium channel currents and its dynamics characteristics in hippocampi and cortices of 2VO rats. These need to be studied further.

Conclusions

MiR-9 plays a key role in regulating the process of Nav1.1/Nav1.2 trafficking via targeting on Nav β 2 protein in 2VO rats at post-transcriptional level, and inhibition of miR-9 may be a potentially-valuable approach to prevent the Nav1.1/Nav1.2 trafficking disturbance induced by CBH.

Methods

Animals

Male Sprague–Dawley rats (weight 220–260 g, obtained from the Animal Centre of the Second Affiliated Hospital of Harbin Medical University, Harbin, Heilongjiang Province, China) were housed at 23 ± 1 °C with 55 ± 5 % of humidity and maintained on 12 h dark–light artificial cycle (lights on at 07:00 A.M.) with food and water available *ad libitum*. Rats used for operation of permanent, bilateral common carotid artery occlusion (2VO) and stereotaxic injection of the lentiviral vectors were anesthetized with chloral hydrate (300 mg/kg, intraperitoneal)

and maintained by administrating 0.5-1.0 % isoflurane. The depth of anesthesia was monitored by detecting reflexes, heart rate and respiratory rate. Samples for qRT-PCR, and Western blot assay were obtained from the hippocampi and cortices of rats after anesthetized with chloral hydrate (500 mg/kg, intraperitoneal) following by confirmation of death by exsanguination. Tissues for primary neuron culturing were from neonatal SD rats after administration of 20 % isoflurane and confirmation of death by cervical dislocation. All animal procedures were approved by the Institutional Animal Care and Use Committee at Harbin Medical University (No.HMUIRB-2008-06) and the Institute of Laboratory Animal Science of China (A5655-01). All procedures were conformed to the Directive 2010/63/EU of the European Parliament.

Permanent, bilateral common carotid artery occlusion (2VO) in the rat

The method for preparation of 2VO rat was according to the previous study [24, 62]. Briefly, after the rats were anaesthetized, the bilateral common carotid arteries of rats were exposed via a midline ventral incision, carefully separated from the vagal nerves, and permanently ligated with 5-0 silk suture. The wound was then closed and rats were allowed recovering from anesthesia before being returned to the animal facility.

Primary hippocampal and cortical neuron culture

The hippocampi and cortices regions were removed from the postnatal day 0 (P0) rat pups. After tissues were dissected and triturated, they were plated onto cell plates precoated with 10 µg/mL poly-D-lysine (Sigma, St Louis, MO, USA) and cultured in the culture media containing neurobasal medium (Gibco, USA) with 2 % B27 supplement (Invitrogen, USA) and 10 % fetal bovine serum (FBS, HyClone, Logan, UT). After 3 days, the neurons were treated with 5 µM cytosine arabinoside (Sigma, St Louis, MO, USA) to inhibit astrocyte proliferation. For all experiments, the neurons were used at 14 days after plating [24].

Synthesis of miR-9, AMO (anti-microRNA antisense oligodeoxyribonucleotide)-miR-9 and other various oligonucleotides

MiR-9 mimics (sense: 5'-UCUUUGGUAUCUAGCUGUAUGA-3'; antisense: 5'-AUACAGCUAGAUAACCAAA GAUU-3') and AMO-miR-9 (5'-UCAUACAGCUAGAUACCAAGA-3') were synthesized by Shanghai GenePharma Co., Ltd (Shanghai, China). AMO-9 contains 2'-O-methyl modifications at every base and a 3' C3-containing amino linker. Additionally, a scrambled RNA was used as a negative control (sense: 5'-UUCUCCGAACGUGUCACGUAA-3, and antisense: 5'-ACGUGACAGUUCGGAGAAUU-3'). The Navβ2-masking antisense oligodeoxynucleotides (ODNs) were synthesized by Shanghai

Sangon Biological Engineering Technology and Service Co., Ltd. Navβ2 masking antisense-ODN-1 was 5'-ATGCCTTCGTCTTCTAGCTGC-3'; which masks the binding sites of miR-9, located in the position 336-358 of SCN2B CDS (coding sequence) region; Navβ2 masking antisense-ODN-2 was 5'TCCTCTTCGGCTTCAGGTC A-3', which masks the binding sites of miR-9, located in the position of 575-597 of SCN2B CDS region. Five nucleotides or deoxynucleotides at both ends of the antisense molecules were locked by a methylene bridge connecting between the 2'-O- and the 4'-C atoms.

Transfection procedures

Thirty pmol/mL miR-9 and/or AMO-9, ODNs or NC siRNAs were transfected into neonatal hippocampal and cortical neurons with X-treme GENE siRNA transfection reagent (Cat.#04476093001, Roche, USA) according to the manufacturer's instructions. Forty-eight hours after transfection, cells were collected for total RNA isolation or protein purification.

Construction of lentivirus vectors

Using the BLOCK-iT polIII miR-RNAi expression vector with the EmGFP kit from invitrogen, three single-stranded DNA oligonucleotides were designed as follows: (1) pre-miR-9 ("top strand" oligo: TGCTGTcTTTggTTaTcTagcTgTaTgaGTTTTGGCCACTGACTGACTcaTcacagagaTaaccaaaga) and its complementary chain ("bottom strand" oligo: CCTGTcTTTggTTaTcTgTaTgaGT CAGTCAGTGGCCAAAACtaTacagcTagaTaaccaaagaC); (2) pre-AMO-miR-9 ("top strand" oligo: TGCTGTcaTcacagcTagaTaaccaaagaGTTTTGGCCACTGACTGACTcTT TggTTcTtagcTgTaTga) and its complement ("bottom strand" oligo: CCTGTcaTcacagcTagaaccaagaGTCAGTC AGTGGCCAAAACtTTTggTTaTcTagcTgTaTgaC); (3) negative control ("top strand" oligo: tgctgAAATGTA CTGCGCGTGGAGACGTTTTGGCCACTGACTGAC GTCTCCACGCAGTACATTT) and its complement ("bottom strand" oligo: cctgAAATGTACTGCGTGGA GACGTCAAGTCAGTGGCCAAAACGTCTCCACGCG CAGTACATTTc). We then cloned the double-stranded oligonucleotides (ds oligo) generated by annealing the top and bottom strand oligos into the pcDNA[™]6.2-GW/± EmGFP-miR vector and transformed the ligated mixture into competent E. coli. After colony was purified and identified as the correct expression clone, the pre-microRNA expression cassette was transferred to other Gateway[®] adapted destination vectors utilizing PolIII promoters and formed a new miRNA expression clone containing attR substrates. The vector was identified after analyzing the plasmid sequence (Invitrogen, USA). The titers of the vectors used for experiments were 9.25×10^8 transducing U/ml. Virus suspensions were

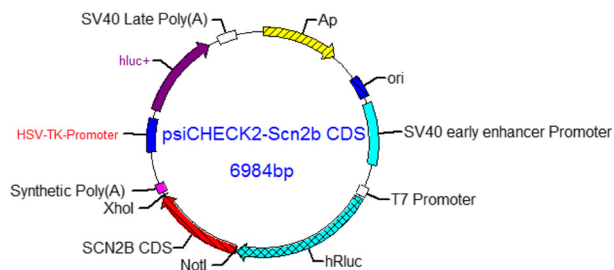
stored at -80°C until use and were briefly centrifuged and kept on ice immediately before injection.

Stereotaxic injection of the lentiviral vectors

After anaesthetized, rats were placed onto a stereotaxic frame (RWB Life Science Co. Ltd, China) described as previous study [24]. Injection coordinates relative to the bregma were as follows: AP (anteroposterior), -4.52 mm ; ML (mediolateral), $\pm 3.2\text{ mm}$; DV (dorsoventral), -3.16 mm below the surface of dura using coordinates derived from the atlas of Paxinos and Watson. Two microliters ($10,000\text{ Tu}/\mu\text{l}$) lenti-pre-miR-9 and/or Lenti-pre-AMO-miR-9 were injected into CA1 of the hippocampus using a $5\ \mu\text{l}$ Hamilton syringe with a 33-gauge tip needle (Hamilton, Bonaduz, Switzerland). The needle was then maintained in the place for another 2 min after injection and then withdrawn very slowly to prevent the solution backflow.

Dual luciferase reporter assay

Before the luciferase activity assay, plasmid design and construction was shown as in the below figure: a 707 bp fragment from the coding region of SCN2B containing the putative binding sequences for miR-9 (position 336–358 and position 575–597 of SCN2B CDS) was amplified by PCR, cloned into the psiCHECK-2-control vector.



Mutagenesis nucleotides were carried out using direct oligomer synthesis for the CDS region of Nav β 2-binding site 1 and Nav β 2-binding site 2. Point mutations were introduced into a possible miR-9 binding site located in the coding region of SCN2B (position 336–358 and position 575–597 of SCN2B CDS). MutSCN2B-1 represents that “GACGAAGG” was mutated “ATCGATCG” in the position 336–358 of SCN2B CDS, MutSCN2B-2 represents that “GACCGAAG” was mutated “ATCGATCG” in the position 575–597 of SCN2B CDS. MutSCN2B-1&2 represents that both sites were mutated. All constructs were sequence verified. Rat SCN2B CDS and mutSCN2B CDS sequences were shown as following: SCN2B CDS sequences (bold nucleotide showed the putative binding sequences for miR-9): ATGCACAGGGATGCCTGGC TACCTCGCCCTGCCTTCAGCCTCACGGGGCTCAG TCTGTTTTTCTCTTTGGTGCCCTCGGGGCGGAG CATGGAAGTCACAGTCCCCACCACTCTTAGTGTC CTCAACGGGTCTGATACCCGCTGCCCTGTACCTT

CAACTCCTGCTATACCGTGAACCACAAGCAGTTC TCTCTGAACTGGACTTACCAGGAGTGTAGCAATT GCTCAGAGGAGATGTTCCCTCCAGTTCCGAATGAA GATCATCAACCTGAAGCTGGAGCGGTTTGGAGA CCGCGTAGAGTTCTCGGGGAACCCAGTAGTAC GACGTGTCAGTGACTCTAAAGAA(CGTGCAGCTA GAAGACGAAGGC)ATTTACAACCTGCTAATCACC AACCTCCAGACCGCCACCGTGGCCATGGCAA GATCTACCTGCAGGTCCTTCTAGAAGGCCCCCA GAGCGGGACTCCACGGTGGCAGTCATCGTGGG TGCTCAGTGGGGGGTTTTCTGGCTGTGGTCA TCTTGGTGCTGATGGTGGTCAAATGTGTGAGG AGAAAAAAGAGCAGAAGCTGAGC(ACGGATG ACCTGAA**GACCGAAGA**)GGAAGGCAAGACGGA TGCGGAGGGCAACGCGGAAGATGGCGCCAAGT AACCGGAAGCTTGCCCTGAAGCCCCTTCTGT GTCTGTCTCTCTCACTCTCTGCCCTGT; mut CN2B CDS (bold nucleotide): ATGCACAGGGATG CCTGGCTACCTCGCCCTGCCTTCAGCCTCACGG GGCTCAGTCTGTTTTTCTCTTTGGTGCCCTCGG GGCGGAGCATGGAAGTCACAGTCCCCACCACT CTAGTGTCTCAACGGGTCTGATACCCGCTG CCCTGTACCTTCAACTCTGCTATAACCGTGAAC CACAAGCAGTTCTCTCTGAACTGGACTTACCA GGAGTGTAGCAATTGCTCAGAGGAGATGTTCC TCCAGTTCGAATGAAGATCATCAACCTGAAGC TGAGAGCGGTTTGGAGACCGCGTAGAGTTCTCG GGAAACCCAGTAAGTACGACGTGTCAGTGAC TCTAAAGAA(CGTGCAGCTAGAA**ATCGATCGC**) ATTTACAACCTGCTACATCACCAACCTCCAGAC CGCCACCGTGGCCATGGCAAGATCTACCTGCA GGTCTTCTAGAAGTGCCCCCAGAGCGGGACT CCACGGTGGCAGTCATCGTGGGTGCCCTCAGTG GGGGGTTTTCTGGCTGTGGTCACTTTGGTGCT GATGGTGGTCAAATGTGTGAGGAGAAAAAAG AGCAGAAGCTGAGC(ACGGATGACCTGAA**ATCG ATCGA**)GGAAGGCAAGACGGATGGCGAGGGCA ACGCGGAAGATGGCGCCAAGTAACCGGAAGCT TGCCCTGAAGCCCCTTCTGTGCTCTCTCTCTCCT CACTCTCTGCCCTGT

The sequence of miR-9 mimic is 5'-UCUUUGGUUUAU CUAGCUGUAUGA-3' (synthesized based on the sequence of rno miR-9 (miRBase Accession No. MIMAT0000781)); that of miR-NC is 5'-UUCUCCGAACGUGUCACGU AA-3'; the sequence of the antisense 2'-O-methyl (2'-O-Me) oligonucleotide for miR-9 is 5'-UCAUACAGC UAGAUAAACCAAAGA-3'; that of inhibitor-NC is 5'-UUCUCCGAACGUGUCACGUTT-3'; HEK293T cells (plated at 40 % ~ 50 % confluence) were transfected with 20 $\mu\text{mol/l}$ miR-9, AMO-miR-9, or negative control siRNAs (NC) as well as 0.5 μg of psi-CHECKTM-2-target DNA (firefly luciferase vector) and 1 μl blank plasmid using lipofectamine 2000 (Invitrogen, USA) transfection reagent according to the manufacturer's instructions. After

48 h of transfection, Firefly and renilla luciferase activities, as indicated by relative luminescence units (RLU) were determined using luciferase assay kits (Cat.#E1910, Promega, USA) and luminometer (GloMaxTM 20/20, Promega, USA) according to the manufacturer's instructions.

Quantitative real-time PCR- (qRT-PCR)

Total RNA was purified with the Trizol Reagent (Invitrogen, USA), according to the manufacturer's instructions as described previously [24]. *MiR-9* level was quantified by the TaqMan[®] MicroRNA Reverse Transcription Kit (Cat.# 000583, ABI, Roche, Branchburg, NJ) and the TaqMan[®] Gene Expression Master Mix (Cat.# 1108123, Applied Biosystems). The TaqMan qRT-PCR probes and primers for *miR-9*, were designed by Applied Biosystems [63]. U6 was used as an internal control. The SYBR Green PCR Master Mix Kit (Applied Biosystems, Cat#4309155) was used for real-time PCR to quantify the *SCN2B* mRNA in our study. β -actin was used as an internal control. Primers are as following: *SCN2B* forward: CTCTCTGAACTGGACTTACC and *SCN2B* reverse: GGTGTTGGTATGTAGCAGTTG; β -actin forward: GGAAATCGTGCGTGACATTA and β -actin reverse: AGGAAGGAAGGCTGGAAGAG. All reactions were performed in triplicate, and the expressions of microRNAs data were shown as Delta-Delta Ct method.

Western blot

Both the total protein and surface protein samples were extracted from hippocampi and cortices of rats or primary cultured neurons for immunoblotting analysis. For the total protein analysis, frozen tissue was homogenized with 1000 μ l solution contained 40 % SDS, 60 % RIPA and 1 % protease inhibitor in each 200 mg brain tissue. The homogenate was then centrifuged at 13,500 rpm for 30 min and the supernatants (containing cytosolic and membrane fractions) were collected. The method of surface protein extraction was using Mem-PER Eukaryotic Membrane Protein Extraction Reagent Kit (Cat# 89826, Pierce Biotechnology, USA) according to the manufacturer's instructions. Protein concentrations were measured spectrophotometrically using a BCA kit (Universal Microplate Spectrophotometer; Bio-Tek Instruments, Winooski, VT, USA). Protein samples were fractionated by SDS-PAGE (10 % polyacrylamide gels for sodium channels) then transferred to PVDF membrane. The primary anti-Nav1.1, Nav1.2, Nav β 2 antibodies (Cat# ASC-001,1:200, RRID:AB_2040003; Cat# ASC-002,1:200, RRID:AB_2040005; Cat# ASC-007, 1:200, RRID:AB_2040011, Alomone Labs, Jerusalem, Israel) were used and β -actin (Kangcheng, Shanghai, China) β -actin (Kangcheng, Shanghai, China) was selected as an internal control of total proteins, mouse anti-human transferrin receptor (TfR) (Cat# 13-6800, RRID:AB_2040011, Invitrogen,

USA) was selected as an internal control of surface proteins. Western blot bands were captured on the Odyssey Infrared Imaging System (LI-COR Biosciences, Lincoln, NE, USA) and quantified with Odyssey v1.2 software by measuring the band intensity (area \times OD) in each group and normalizing to the internal control.

Immunocytochemistry staining

The cultured neonatal rat neurons were transcardially perfused by 4 % buffered paraformaldehyde, pH7.4. After blocking, cultured neonatal rat neurons were incubated with the anti- β -Tubulin III (neuronal) antibody (Cat no. T8578; 1:5000; Sigma, Saint Louis, USA) or anti-Nav1.1, Nav1.2, Nav β 2 antibodies (Alomone Labs, Jerusalem, Israel) overnight at 4 °C, and then the cultured neonatal rat neurons were washed and incubated with the secondary antibodies conjugated to Alexa Fluor 488 and Alexa Fluor 594 (Molecular Probes, Eugene, OR, USA) for 1 h at room temperature.

Statistical analysis

Data were described as mean \pm s.e.m for experimental data. The two-tailed Student's *t*-test was applied for comparisons between the two groups. Multi-group's comparisons were performed by One-way ANOVA. SPSS19.0 software was used for all statistical analyses. $P < 0.05$ was considered significant.

Abbreviations

VGSC: Voltage-gated sodium channel; AD: Alzheimer's disease; CBH: Chronic brain hypoperfusion; CNS: Central nerve system; 2VO: Bilateral common carotid artery occlusion; ODNs: Oligodeoxynucleotides; AMO: Anti-microRNA antisense oligodeoxyribonucleotide; CDS: Coding sequence; TfR: Transferrin receptor; AIS: Axon initial segment; q-RT-PCR: Quantitative real-time PCR.

Competing interests

The authors declare that they have no competing interests.

Authors' contributions

LHS, JA conceived and designed the experiments, performed experiments, were involved in drafting and editing the manuscript, and interpreted primary data. XLH, MLY, LWP, HC, YNB, FG, TL, XC performed the experiments. RZ, TB, NW edited the manuscript. HLL, XH contributed reagents. All authors read and approved the final manuscript.

Acknowledgments

This work was supported by the research funds from Creative Research Groups of the National Natural Science Foundation of China (81121003) and Natural Science Foundation of China (81371211, 81000499, 81271207 and 81471115) and partially supported by the Special research Grants from Postdoctoral Science Foundation of China (2012 T50376) and Postdoctoral Science Foundation of Heilongjiang province (LBH-Q13108, LBH-z13155).

Author details

¹Department of Pharmacology, Harbin Medical University, No.157 Baojian Road, Nangang District, Harbin, Heilongjiang Province 15008, China.

²Department of Neurosurgery, The First Affiliated Hospital of Harbin Medical University, No.157 Baojian Road, Nangang District, Harbin, Heilongjiang Province 150081, China.

Received: 25 November 2014 Accepted: 24 July 2015

Published online: 11 August 2015

References

- Brackenbury WJ, Isom LL. Na Channel beta Subunits: Overachievers of the Ion Channel Family. *Front Pharmacol.* 2011;2:53.
- Eijkelkamp N, Linley JE, Baker MD, Minett MS, Cregg R, Werdehausen R, et al. Neurological perspectives on voltage-gated sodium channels. *Brain.* 2012;135:2585–612.
- Abdelsayed M, Sokolov S. Voltage-gated sodium channels: pharmaceutical targets via anticonvulsants to treat epileptic syndromes. *Channels (Austin).* 2013;7:146–52.
- Mantegazza M, Curia G, Biagini G, Ragsdale DS, Avoli M. Voltage-gated sodium channels as therapeutic targets in epilepsy and other neurological disorders. *Lancet Neurol.* 2010;9:413–24.
- Tarnawa I, Bolcskei H, Kocsis P. Blockers of voltage-gated sodium channels for the treatment of central nervous system diseases. *Recent Pat CNS Drug Discov.* 2007;2:57–78.
- Amatniek JC, Hauser WA, DelCastillo-Castaneda C, Jacobs DM, Marder K, Bell K, et al. Incidence and predictors of seizures in patients with Alzheimer's disease. *Epilepsia.* 2006;47:867–72.
- Bakker A, Krauss GL, Albert MS, Speck CL, Jones LR, Stark CE, et al. Reduction of hippocampal hyperactivity improves cognition in amnesic mild cognitive impairment. *Neuron.* 2012;74:467–74.
- Sanchez PE, Zhu L, Verret L, Vossel KA, Orr AG, Cirrito JR, et al. Levetiracetam suppresses neuronal network dysfunction and reverses synaptic and cognitive deficits in an Alzheimer's disease model. *Proc Natl Acad Sci U S A.* 2012;109:E2895–2903.
- Palop JJ, Mucke L. Epilepsy and cognitive impairments in Alzheimer disease. *Arch Neurol.* 2009;66:435–40.
- Born HA, Kim JY, Savjani RR, Das P, Dabaghian YA, Guo Q, et al. Genetic suppression of transgenic APP rescues Hypersynchronous network activity in a mouse model of Alzheimer's disease. *J Neurosci.* 2014;34:3826–40.
- Bender AC, Morse RP, Scott RC, Holmes GL, Lenck-Santini PP. SCN1A mutations in Dravet syndrome: impact of interneuron dysfunction on neural networks and cognitive outcome. *Epilepsy Behav.* 2012;23:177–86.
- Kim DY, Carey BW, Wang H, Ingano LA, Binshtok AM, Wertz MH, et al. BACE1 regulates voltage-gated sodium channels and neuronal activity. *Nat Cell Biol.* 2007;9:755–64.
- Verret L, Mann EO, Hang GB, Barth AM, Cobos I, Ho K, et al. Inhibitory interneuron deficit links altered network activity and cognitive dysfunction in Alzheimer model. *Cell.* 2012;149:708–21.
- Hu X, Zhou X, He W, Yang J, Xiong W, Wong P, et al. BACE1 deficiency causes altered neuronal activity and neurodegeneration. *J Neurosci.* 2010;30:8819–29.
- Maschietto M, Girardi S, Dal Maschio M, Scorsetto M, Vassanelli S. Sodium channel beta2 subunit promotes filopodia-like processes and expansion of the dendritic tree in developing rat hippocampal neurons. *Front Cell Neurosci.* 2013;7:2.
- Chen C, Calhoun JD, Zhang Y, Lopez-Santiago L, Zhou N, Davis TH, et al. Identification of the cysteine residue responsible for disulfide linkage of Na⁺ channel alpha and beta2 subunits. *J Biol Chem.* 2012;287:39061–9.
- Isom LL, Ragsdale DS, De Jongh KS, Westenbroek RE, Reber BF, Scheuer T, et al. Structure and function of the beta 2 subunit of brain sodium channels, a transmembrane glycoprotein with a CAM motif. *Cell.* 1995;83:433–42.
- Chen C, Bharucha V, Chen Y, Westenbroek RE, Brown A, Malhotra JD, et al. Reduced sodium channel density, altered voltage dependence of inactivation, and increased susceptibility to seizures in mice lacking sodium channel beta 2-subunits. *Proc Natl Acad Sci U S A.* 2002;99:17072–7.
- Huth T, Alzheimer C. Voltage-dependent Na⁺ channels as targets of BACE1 - implications for neuronal firing and beyond. *Curr Alzheimer C.* 2012;9: 184–8.
- Corbett BF, Leiser SC, Ling HP, Nagy R, Breyse N, Zhang X, et al. Sodium channel cleavage is associated with aberrant neuronal activity and cognitive deficits in a mouse model of Alzheimer's disease. *J Neurosci.* 2013;33: 7020–6.
- Kitaguchi H, Tomimoto H, Ihara M, Shibata M, Uemura K, Kalaria RN, et al. Chronic cerebral hypoperfusion accelerates amyloid beta deposition in APPSwInd transgenic mice. *Brain Res.* 2009;1294:202–10.
- Zhiyou C, Yong Y, Shanquan S, Jun Z, Liangguo H, Ling Y, et al. Upregulation of BACE1 and beta-amyloid protein mediated by chronic cerebral hypoperfusion contributes to cognitive impairment and pathogenesis of Alzheimer's disease. *Neurochem Res.* 2009;34:1226–35.
- Ruitenberg A, den Heijer T, Bakker SL, van Swieten JC, Koudstaal PJ, Hofman A, et al. Cerebral hypoperfusion and clinical onset of dementia: the Rotterdam Study. *Ann Neurol.* 2005;57:789–94.
- Ai J, Sun LH, Che H, Zhang R, Zhang TZ, Wu WC, et al. MicroRNA-195 protects against dementia induced by chronic brain hypoperfusion via its anti-amyloidogenic effect in rats. *J Neurosci.* 2013;33:3989–4001.
- Farkas E, Institoris A, Domoki F, Mihaly A, Bari F. The effect of pre- and posttreatment with diazoxide on the early phase of chronic cerebral hypoperfusion in the rat. *Brain Res.* 2006;1087:168–74.
- Liu HX, Zhang JJ, Zheng P, Zhang Y. Altered expression of MAP-2, GAP-43, and synaptophysin in the hippocampus of rats with chronic cerebral hypoperfusion correlates with cognitive impairment. *Brain Res Mol Brain Res.* 2005;139:169–77.
- Ren L, Wang YK, Fang YN, Zhang AW, Li XL. Effect of electroacupuncture therapy on the expression of Na(v)1.1 and Na(v)1.6 in rat after acute cerebral ischemia. *Neurol Res.* 2010;32:1110–6.
- Deo M, Yu JY, Chung KH, Tippens M, Turner DL. Detection of mammalian microRNA expression by in situ hybridization with RNA oligonucleotides. *Dev Dyn.* 2006;235:2538–48.
- Shibata M, Nakao H, Kiyonari H, Abe T, Aizawa S. MicroRNA-9 regulates neurogenesis in mouse telencephalon by targeting multiple transcription factors. *J Neurosci.* 2011;31:3407–22.
- Hu Y, Luo M, Ni N, Den Y, Xia J, Chen J, et al. Reciprocal Actions of microRNA-9 and TLX in the Proliferation and Differentiation of Retinal Progenitor Cells. *Stem Cells Dev.* 2014;23(22):2771–81.
- Zhao C, Sun G, Li S, Shi Y. A feedback regulatory loop involving microRNA-9 and nuclear receptor TLX in neural stem cell fate determination. *Nat Struct Mol Biol.* 2009;16:365–71.
- Pietrzykowski AZ, Friesen RM, Martin GE, Puig SI, Nowak CL, Wynne PM, et al. Posttranscriptional regulation of BK channel splice variant stability by miR-9 underlies neuroadaptation to alcohol. *Neuron.* 2008;59:274–87.
- Coolen M, Thieffry D, Drivenes O, Becker TS, Bally-Cuif L. miR-9 controls the timing of neurogenesis through the direct inhibition of antagonistic factors. *Dev Cell.* 2012;22:1052–64.
- Zhao C, Sun G, Ye P, Li S, Shi Y. MicroRNA let-7d regulates the TLX/microRNA-9 cascade to control neural cell fate and neurogenesis. *Sci Rep.* 2013;3:1329.
- Tan X, Wang S, Yang B, Zhu L, Yin B, Chao T, et al. The CREB-miR-9 negative feedback microcircuitry coordinates the migration and proliferation of glioma cells. *PLoS One.* 2012;7:e49570.
- Dajas-Bailador F, Bonev B, Garcez P, Stanley P, Guillemot F, Papalopulu N: microRNA-9 regulates axon extension and branching by targeting Map1b in mouse cortical neurons. *Nat Neurosci.* 2012;15:697–699.
- Otaegi G, Pollock A, Sun T. An Optimized Sponge for microRNA miR-9 Affects Spinal Motor Neuron Development in vivo. *Front Neurosci.* 2011;5:146.
- Packer AN, Xing Y, Harper SQ, Jones L, Davidson BL. The bifunctional microRNA miR-9/miR-9* regulates REST and CoREST and is downregulated in Huntington's disease. *J Neurosci.* 2008;28:14341–6.
- Lukiw WJ. Micro-RNA speciation in fetal, adult and Alzheimer's disease hippocampus. *Neuroreport.* 2007;18:297–300.
- Lai HC, Jan LY. The distribution and targeting of neuronal voltage-gated ion channels. *Nat Rev Neurosci.* 2006;7:548–62.
- Saba R, Schrat GM. MicroRNAs in neuronal development, function and dysfunction. *Brain Res.* 2010;1338:3–13.
- Lewis BP, Burge CB, Bartel DP. Conserved seed pairing, often flanked by adenosines, indicates that thousands of human genes are microRNA targets. *Cell.* 2005;120:15–20.
- Reczko M, Maragkakis M, Alexiou P, Grosse I, Hatzigeorgiou AG. Functional microRNA targets in protein coding sequences. *Bioinformatics.* 2012;28: 771–6.
- Ogata N, Ohishi Y. Molecular diversity of structure and function of the voltage-gated Na⁺ channels. *Jpn J Pharmacol.* 2002;88:365–77.
- Leterrier C, Brachet A, Fache MP, Dargent B. Voltage-gated sodium channel organization in neurons: protein interactions and trafficking pathways. *Neurosci Lett.* 2010;486:92–100.
- Dufflocq A, Le Bras B, Bullier E, Couraud F, Davenne M. Nav1.1 is predominantly expressed in nodes of Ranvier and axon initial segments. *Mol Cell Neurosci.* 2008;39:180–92.
- Lorincz A, Nusser Z. Cell-type-dependent molecular composition of the axon initial segment. *J Neurosci.* 2008;28:14329–40.

48. Kim DY, Gersbacher MT, Inquimbert P, Kovacs DM. Reduced sodium channel Na(v)1.1 levels in BACE1-null mice. *J Biol Chem*. 2011;286:8106–16.
49. Kovacs DM, Gersbacher MT, Kim DY. Alzheimer's secretases regulate voltage-gated sodium channels. *Neurosci Lett*. 2010;486:68–72.
50. Gersbacher MT, Kim DY, Bhattacharyya R, Kovacs DM. Identification of BACE1 cleavage sites in human voltage-gated sodium channel beta 2 subunit. *Mol Neurodegener*. 2010;5:61.
51. Diakov A, Bera K, Mokrushina M, Krueger B, Korbmacher C. Cleavage in the {gamma}-subunit of the epithelial sodium channel (ENaC) plays an important role in the proteolytic activation of near-silent channels. *J Physiol*. 2008;586:4587–608.
52. Harris M, Firsov D, Vuagniaux G, Stutts MJ, Rossier BC. A novel neutrophil elastase inhibitor prevents elastase activation and surface cleavage of the epithelial sodium channel expressed in *Xenopus laevis* oocytes. *J Biol Chem*. 2007;282:58–64.
53. Kim DY, Ingano LA, Carey BW, Pettingell WH, Kovacs DM. Presenilin/gamma-secretase-mediated cleavage of the voltage-gated sodium channel beta2-subunit regulates cell adhesion and migration. *J Biol Chem*. 2005;280:23251–61.
54. Sethi P, Lukiw WJ. Micro-RNA abundance and stability in human brain: specific alterations in Alzheimer's disease temporal lobe neocortex. *Neurosci Lett*. 2009;459:100–4.
55. Cogswell JP, Ward J, Taylor IA, Waters M, Shi Y, Cannon B, et al. Identification of miRNA changes in Alzheimer's disease brain and CSF yields putative biomarkers and insights into disease pathways. *J Alzheimers Dis*. 2008;14:27–41.
56. Schonrock N, Humphreys DT, Preiss T, Gotz J. Target gene repression mediated by miRNAs miR-181c and miR-9 both of which are down-regulated by amyloid-beta. *J Mol Neurosci*. 2012;46:324–35.
57. Duursma AM, Kedde M, Schrier M, le Sage C, Agami R. miR-148 targets human DNMT3b protein coding region. *RNA*. 2008;14:872–7.
58. Zhou X, Duan X, Qian J, Li F. Abundant conserved microRNA target sites in the 5'-untranslated region and coding sequence. *Genetica*. 2009;137:159–64.
59. Huang S, Wu S, Ding J, Lin J, Wei L, Gu J, et al. MicroRNA-181a modulates gene expression of zinc finger family members by directly targeting their coding regions. *Nucleic acids Res*. 2010;38:7211–8.
60. Goswami S, Tarapore RS, Teslaa JJ, Grinblat Y, Setaluri V, Spiegelman VS. MicroRNA-340-mediated degradation of microphthalmia-associated transcription factor mRNA is inhibited by the coding region determinant-binding protein. *Biol Chem*. 2010;285:20532–40.
61. Long Q, Johnson BA, Osunkoya AO, Lai YH, Zhou W, Abramovitz M, et al. Protein-coding and microRNA biomarkers of recurrence of prostate cancer following radical prostatectomy. *Am J Pathol*. 2011;179:46–54.
62. Kumaran D, Udayabanu M, Kumar M, Aneja R, Katyal A. Involvement of angiotensin converting enzyme in cerebral hypoperfusion induced anterograde memory impairment and cholinergic dysfunction in rats. *Neuroscience*. 2008;155:626–39.
63. Zhuang G, Wu X, Jiang Z, Kasman I, Yao J, Guan Y, et al. Tumour-secreted miR-9 promotes endothelial cell migration and angiogenesis by activating the JAK-STAT pathway. *EMBO J*. 2012;31:3513–23.

Submit your next manuscript to BioMed Central and take full advantage of:

- Convenient online submission
- Thorough peer review
- No space constraints or color figure charges
- Immediate publication on acceptance
- Inclusion in PubMed, CAS, Scopus and Google Scholar
- Research which is freely available for redistribution

Submit your manuscript at
www.biomedcentral.com/submit

